JPMB | Journal of Plant Molecular Breeding
Published by Genetics and Agricultural Biotechnology Institute of Tabarestan
2025 | Volume 13 | Issue 1

Original paper

Green synthesis of gold nanoparticles using aqueous extract of *Haplophyllum canaliculatum* Boiss and its antioxidant activity

Niloofar Ahadi[1], Kambiz Larijani[1], Lida Ghaderi [2,*], Parvin Asen [3,*]

1. Department of Chemistry, Science and Research Branch, Islamic Azad University, Tehran , Iran
2. Faculty of Medicinal Plants, Amol University of Special Modern Technologies, Amol, Iran
3. Department of Nano Biotechnology, Faculty of Biotechnology, Amol University of Special Modern Technologies, Amol 46158-63111, Iran

Abstract: Green synthesis of gold nanoparticles (AuNPs) is increasingly popular due to their broad potential applications. Hence, this research reports the synthesis of AuNPs by reducing of $HAuCl_4$ using an aqueous extract of *Haplophyllum canaliculatum* Boiss as both a reducing and stabilizing agent. In addition, the antioxidant activity of as-prepared AuNPs was investigated. The physicochemical properties of AuNPs were characterized by UV-visible (UV-Vis) spectroscopy, Fourier transform infrared spectroscopy (FT-IR), X-ray diffraction (XRD), and field emission scanning electron microscopy (FESEM). The UV-Vis spectra displayed a surface plasmon resonance band at 523 nm, which confirmed the formation of AuNPs. Also, the FESEM image revealed that the particle sizes of the AuNPs ranged from 15 to 25 nm. In addition, the Debye-Scherrer equation showed a particle size of 16.4 nm from the XRD result. Furthermore, the biosynthesized AuNPs exhibited significant antioxidant activity ($P< 0.05$) against DPPH free radicals' scavenger in a concentration-dependent manner. The IC_{50} value of the AuNPs was obtained as 44.42 µg mL^{-1}. The antioxidant activity of the AuNPs likely stems from secondary metabolites of the *H. canaliculatum* extract, such as quinoline alkaloids. These findings offer a promising approach for developing biosynthesized AuNPs for potential pharmaceutical applications.

Keywords: Green synthesis, gold nanoparticles, *Haplophyllum canaliculatum*, antioxidant activity.

OPEN ACCESS

Edited by

Dr. Pouria Biparva,
Department of Basic Sciences, Faculty of Agricultural Sciences, Sari University of Agricultural Sciences and Natural Resources, Sari.

Date

Received: 17 April 2025
Accepted: 14 May 2025
Published: 22 May 2025

Correspondence

Dr. Lida Ghaderi
l.ghaderi@ausmt.ac.ir
Dr. Parvin Asen
parvinasen@ausmt.ac.ir

Citation

Ahadi, N., Larijani , K., Ghaderi, L., and Asen, P. (2025). Green synthesis of gold nanoparticles using aqueous extract of *Haplophyllum canaliculatum* Boiss and its antioxidant activity. *J Plant Mol Breed. 13* (1): 71-80.
doi: 10.22058/jpmb.2025.2058107.1336.

Introduction

Nanomaterials have gained significant attention owing to their promising applications in drug delivery, biomedicine, material chemistry, and pollution control over the past few years (Patil et al., 2023). The high surface-to-volume ratio, small size, shape, charge characteristics, and high reactivity of nanoparticles (NPs) compared to their bulk materials are expected to result in improved performance (Boruah et al., 2021). Metal NPs are nanomaterials consisting of a single metal. Some of the most commonly produced metal NPs include gold (Au), silver (Ag), platinum (Pt), palladium (Pd), copper (Cu), zinc (Zn), ruthenium (Ru), etc. (Saleh, 2022). Among the various metallic NP, AuNPs, have attracted great interest due to their unique intrinsic features, such as optical properties, ease of synthesis, tunable sizes, multifunctional capabilities, and facile surface modification. They are very biocompatible, low in toxicity, relatively inert, and generally stable (Santhosh et al., 2022; Patil et al., 2023). In addition, colloidal Au solutions have achieved increasing attention for studying their cytotoxicity properties, with potential applications in pharmacology, medicine, the food industry, water purification, etc. They have a wide range of biological applications, including labeling, drug delivery, photothermal therapy, tissue/tumor imaging, and sensing (Saleh, 2022). There are various approaches for the synthesis of AuNPs such as chemical reduction methods, lithography, and physical methods. However, these methods have several drawbacks including the use of biological toxic chemicals, ecological imbalance, high processing cost, and the potential to create a toxic environment (Ghasemi et al., 2025). Therefore, developing a novel and green process to synthesize the AuNPs is essential. In recent years, the biological synthesis of AuNPs utilizing plants, algae, fungi, and microorganisms has become preferred because these methods decrease the drawbacks of previously mentioned methods (Boruah et al., 2021; Chen et al., 2021). Plant-based synthesis of nanoparticles offers more advantages than other biological methods, including the elimination of the need to maintain microbial cultures and being more cost-effective for large-scale nanoparticle production (Sujitha and Kannan, 2013; Ghasemi et al., 2025).

Different parts of plants such as leaves, fruits, bark, flowers, peels, seeds, rhizomes, and roots can be used for the biosynthesis of AuNPs. The constituents extracted from roots and above-ground plant parts of medicinal plants contain various secondary metabolites also known as phytochemicals such as phenolic compounds (e.g., polyphenols, flavonoids, tannins, and lignans), terpenoids, quinones, coumarins, alkaloids, saponins, steroids, and glycosides (Arzani et al., 2025). They have multiple health-promoting benefits to animals and human, especially as antioxidants, antimicrobials, anticarcinogens, and the suppression of inflammatory responses (Mohammadinejad et al., 2019), and also act as both reducing and stabilizing agents (Saleh, 2022). Biosynthesis of AuNPs by plants such as *Curcumae kwangsiensis*, *Moringa oleifera*, *Glaucium flavum*, *Stevia rebaudiana*, and *Plumeria alba* have been reported (Boruah et al., 2021; Chen et al., 2021; Santhosh et al., 2022). *Haplophyllum canaliculatum* (*H. canaliculatum*) Boiss. member of the Rutaceae family, is an endemic species of Iran primarily distributed in southeastern mountainous regions. The genus *Haplophyllum* contains essential oils, alkaloids, fixed oils, coumarins, sterols, flavonoids, and lignans (Varamini et al., 2009; Mohammadhosseini et al., 2021). It has been reported that *Haplophyllum* spp. has various pharmacological activities including antioxidant, cytotoxic, anti-leishmanial, and anti-inflammatory properties (Nikbakht et al., 2016). Varamini et al. isolated five quinoline alkaloids from the methanolic extract of *H. canaliculatum*, namely 7-isopentenyloxy-γ-fagarine, atanine, skimmianine, flindersine, and perfamine (Varamini et al., 2009). Previous studies have demonstrated that secondary metabolites, including phenolic acids, alkaloids, flavonoids, and terpenoids, commonly found in plant extracts, contribute to the reduction of NPs and improve their stability (Fatima et al., 2024). To the best of our knowledge, the use of *H. canaliculatum* extract for the biosynthesis of AuNPs has not been explored. Inspired by the above discussions, we presented the green synthesis of AuNPs using an aqueous extract of *Haplophyllum canaliculatum* to investigate the antioxidant activity.

Materials and Methods

Materials

Hydrogen tetrachloroaurate (iii) trihydrate (HAuCl4. 3H2O; ⩾ 99.9 %), polyvinylpyrrolidone (PVP), 2,2-diphenyl-1-picrylhydrazyl (DPPH ⩾ 98 %), ascorbic acid (C6H8O6) and methanol (CH3OH, ⩾ 99.9 %) were purchased from Sigma Aldrich. The aerial parts of *H. canaliculatum* were collected from an altitude of 1300 meters of Tang Zagh Mountains with 27°933'44'' latitude and 55°916'66'' longitude in Hormozgan province, Iran in November 2022.

Preparation of the extract

The aerial parts of *H. canaliculatum* were air-dried in the shade environment at room temperature and finely powdered using a household mixer. Then, 10 g of the plant powder was mixed with 100 mL of deionized water and stirred at 45°C for 60 min. After stirring, the supernatant was collected by Whatman No. 1 filter paper. The obtained extract was stored at 4°C for further experiments.

Synthesis of AuNPs

The aqueous solution of $HAuCl_4$ with a concentration of 1 mM was prepared. 0.004 g of PVP was added to 1 mM of $HAuCl_4$ solution as a capping and soft reducing agent (Ismillayli et al., 2024; Ortega-Cordova et al., 2024). Then, the mixture was stirred at 60°C using a magnetic hotplate stirrer for 1 h. Then, 1 mL of plant extract was added dropwise to the stirring solution. The color change from yellow to purple during the reaction was observed, which confirms the synthesis of the AuNPs. The resulting AuNPs solution was centrifuged at 13000 rpm for 15 min. The collected AuNPs were rinsed three times with deionized water.

Materials characterization

The absorbance spectra of AuNPs were characterized by a UV-Vis spectrophotometer (Jenway company (6305 model), England). The spectra were monitored by scanning the sample in the200-860 nm range. XRD pattern of AuNPs was obtained by GBC Scientific Equipment Pty Ltd. Australia, using Cu-Ka radiation (λ = 1.54 Å, 40 keV) in the 2Θ range of 10–80° at 25 °C with a scan speed of 10° min^{-1}. FT-IR spectra were carried out within the range of 400-4000 cm^{-1} using an ABB Bomem MB-100 FT-IR spectrophotometer.

The crystallite size of AuNP was calculated through the Deby-Sherrer formula from XRD analysis from follwing equation:

$$D = \frac{0.9\lambda}{\beta \cos\theta} \quad (2)$$

Where D, λ, β, and θ are the nanocrystal diameter, light wavelength, full-width half maximum (FWHM, in radians), and Bragg angle, respectively. The morphology of the as-prepared AuNPs was investigated by field emission scanning electron microscopy (FESEM, MIRA-TESCAN).

Free radical scavenging activity

Free radical scavenging activities of the plant extract, AuNPs, and ascorbic acid (Vit C) as the standard were determined according to the DPPH method of Molyneux (2004) with some modifications. The dried extract and powdered form of AuNPs were obtained using a freeze dryer (OPERON, Korea). Stock solutions of extract, AuNPs and Vit C were prepared at concentration of 10 $mgmL^{-1}$ in distilled water . These stock solutions were then used to prepare different concentrations (31.25, 62.5, 125, 250 μg mL^{-1}) of the extract, AuNPs and Vit C. Then, 80 mg mL^{-1} DPPH solution in methanol was added to an equal volume of various concentrations of extract, AuNPs, and Vit C. The mixtures were incubated in the dark at 25°C for 45 min. After the incubation period, the absorbance of the samples was determined at a wavelength of 517 nm using a spectrophotometer. The percentage of free radical scavenging DPPH (I %) was calculated using the following equation:

$I\% = [(A_{BC}-A_{BS})/A_{BC}] \times 100$ (1)

where A_{BC} is the absorbance of the negative control and A_{BS} is the absorbance of the experimental samples.

Statistical analysis

To ensure a reliable comparison of the results, at least three replicates of each measurement were performed, and the results are presented as mean ± standard deviation. The statistical analysis was performed with one-way analysis of variance (ANOVA) followed by Duncan's multiple range test to identify significant differences between groups. Statistical significance was defined as a *p*-value of less than 0.05.

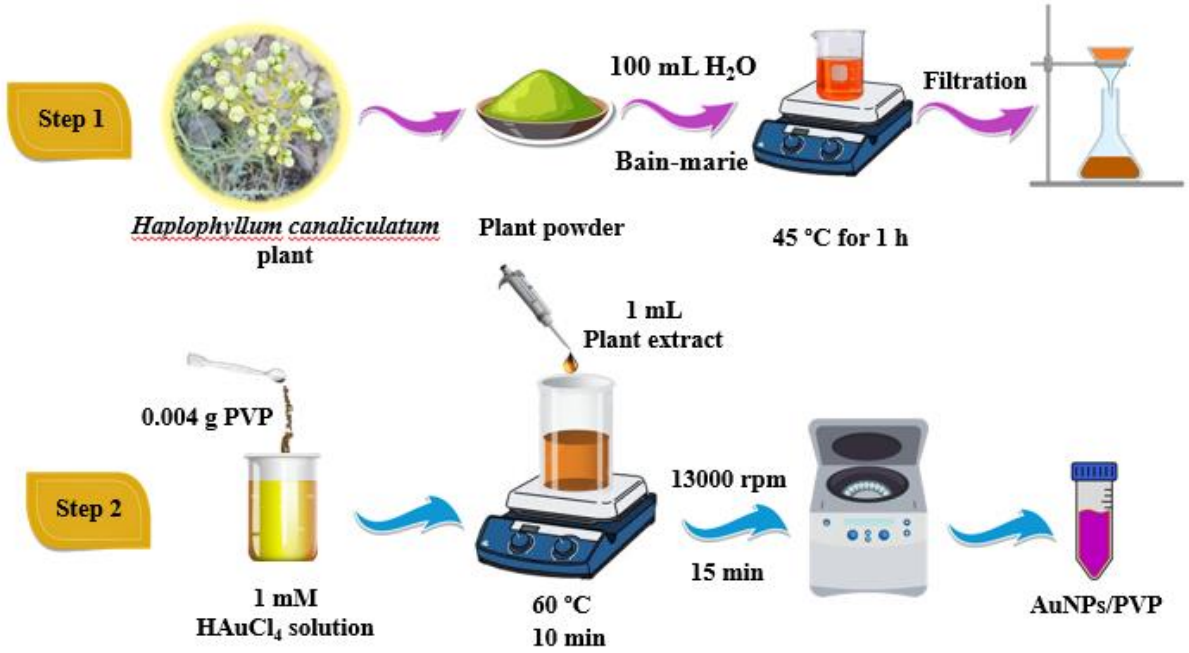

Figure 1. Schematic illustration of the synthetic strategy of AuNPs.

Results

The synthesis of AuNP and its characterization

The green synthesis of the AuNPs is schematically shown in Figure 1.

UV–Vis was carried out to confirm the formation of AuNPs. As shown in Figure 2, the AuNPs exhibited a surface plasmon resonance (SPR) band at 523 nm (Rosyidah et al., 2024).

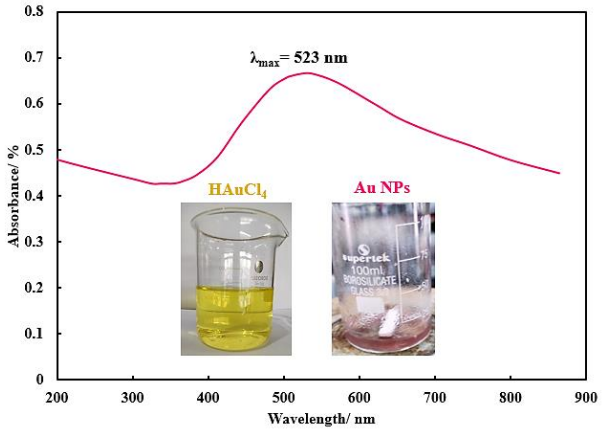

Figure 2. UV-Vis spectrum of AuNPs.

The FT-IR spectroscopy technique was used to characterize the plant extract and AuNPs. As can be seen in Figure 3, the FT-IR spectrum of the plant extract showed the absorption band appearing at 631 cm^{-1}, which can be attributed to the aliphatic C-H bending (Zakaria et al., 2019). The observed peak at 747 cm^{-1} can be ascribed to the out-of-plane bending of C-H. The peaks at 1029 and 1265 cm^{-1} were probably related to the C–O stretching vibrations in esters, alcohols, or ethers (Shehzad et al., 2018). The peak appeared at 1259 cm^{-1} can be ascribed to the C-O-C stretching of functional groups in aldehydes, ketones, or carboxylic acids. The band located at 1405 cm^{-1} can be ascribed to the bending vibrations of O-H bonds in alcohols or carboxylic acids. The peak at 1630 cm^{-1} can be attributed to the stretching vibrations of C=C (Deghiedy and El-Sayed, 2020). The band at 1725 cm^{-1} can be associated with the stretching vibration of C=O (Zidan et al., 2019). The two peaks at 2823 and 2890 cm^{-1} can be attributed to the C-H stretching vibration (Abdelghany et al., 2015). The observed broad band at the region of 3400 cm^{-1} was typically ascribed to the stretching vibrations of H_2O molecules. For AuNPs, the peak at 605 cm^{-1} can be ascribed to aliphatic C-H bending (Zakaria et al.,

2019). The peak located at 720 cm^{-1} was related to the out-of-plane bending of C-H (Tharani et al., 2020). The peak at 1003 was indexed to the stretching vibrations of C-O. The peak at 1265 cm^{-1} can be ascribed to the C-N stretching vibration (Wei et al., 2009). The peak located at 1391 cm^{-1} can be assigned to the bending vibrations of O-H. The observed peak at 1628 cm^{-1} can be ascribed to the stretching vibrations of C=C (Deghiedy and El-Sayed, 2020).

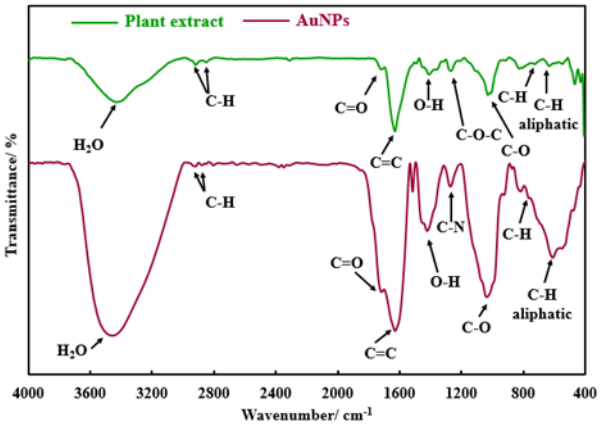

Figure 3. FT-IR spectra of plant extract and AuNPs.

The band at 1711 cm^{-1} belonged to the stretching vibrations of C=O. The peaks at 2872 and 2927 cm^{-1} were attributed to the C-H stretching vibration. The appeared broad band at 3370 cm^{-1} can be related to the stretching vibrations of H_2O. The crystal structure of the as-prepared AuNPs was analyzed by XRD.

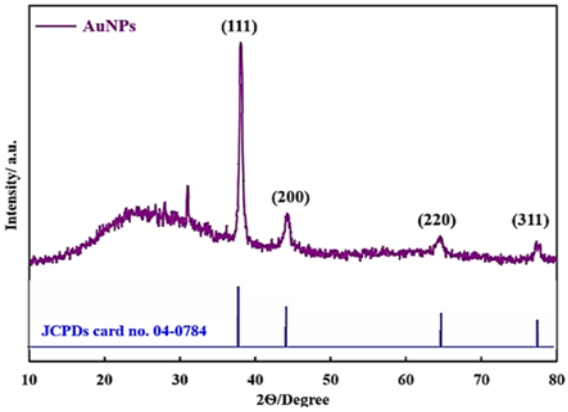

Figure 4. XRD pattern of AuNPs and the corresponing JCPDs card.

Figure 4 exhibits a broad diffraction peak at 2θ = 25.5°, corresponding amorphous PVP (Lv et al., 2019). The diffraction peaks at 38.1°, 44.3°, 65.1°, and 77.7° were attributed to the (111), (200), (220), and (311) crystal planes, indicating the synthesis of AuNPs (JCPDs card no. 04-0784) (Alharbi et al., 2017). Figure 5 shows the SEM image of the AuNPs. The SEM image showed the particle size of AuNPs in the range of 18-25 nm. However, agglomeration of the AuNPs can be observed in some areas from the SEM images.

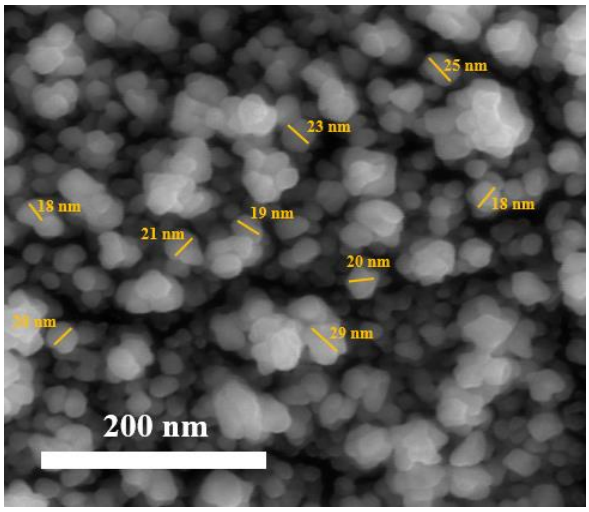

Figure 5. SEM image of AuNPs.

DPPH free radical scavenging activity

The antioxidant activity of the AuNPs and the plant extract was measured by DPPH scavenging assay, with Vit C as the standard (Figure 6). DPPH is a stable violet-colored free radical compound that can accept electrons from antioxidant compounds, resulting in the formation of a yellow hydrazine derivative (Kureshi et al., 2020). The obtained results from the antioxidant activity demonstrated effective free radical inhibition for the AuNPs and the plant extract. As shown in Figure 6, the percentage of DPPH radical scavenging activity exhibited a dose-dependent response for both of them ($P< 0.05$). At the lowest (31.25 μg mL^{-1}) and highest (250 μg mL^{-1}) concentrations, the AuNPs exhibited 46.66±1.65% and 86.33±1.86% inhibitory activities, respectively. Similarly, the plant extract showed 45.83±1.29% and 84.98±1.90% inhibition at concentrations of 31.25 and 250 μg mL^{-1},

respectively. The statistical evaluation revealed no significant difference in antioxidant activ between the extract and AuNPs at the same concentrations (P>0.05).

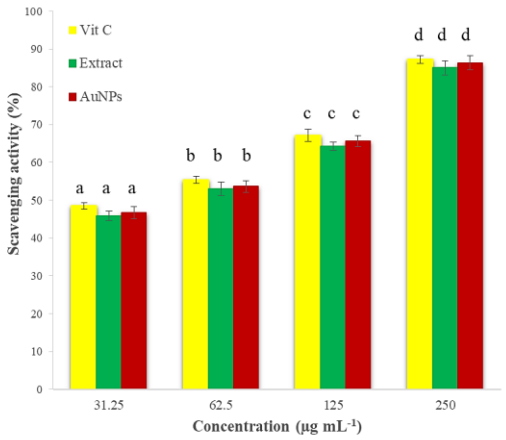

Figure 6. DPPH free radical scavenging activity of the AuNPs and the plant extract (columns with same letter are not significantly different at the 0.05 level).

IC_{50} was determined based on the sample concentration required for 50% scavenging of DPPH radicals (Table 1). Lower values in the test demonstrate greater antioxidant potency of the samples. The IC_{50} value of the AuNPs was determined to 44.42 µg mL^{-1}.

Table 1. IC50 values of the AuNPs, extract, and Vit C (µg mL^{-1}).

Samples	IC_{50} (µg mL^{-1})
Vit C	34.35
AuNPs	44.42
Extract	49.04

Discussion

In general, the preparation of AuNPs involves two main cases: (I) the $HAuCl_4$ releases Au^{3+} ions, which ultimately leads to the formation of AuNPs, (II) the secondary metabolites of plants, such as alkaloids, flavonoids, and terpenoids, can act as reducing agents. These bioactive compounds reduce Au^{3+} ions and facilitate the formation of AuNPs. Also, they play a crucial role in stabilizing the NPs, inhibiting agglomeration, and ensuring a consistent size distribution (Mahajan et al., 2025). In addition, PVP was used as a capping and soft reducing agent for the preparation of stable AuNPs. It can be explained that PVP coordinates with the Au ion through the lone pair electrons of the oxygen atoms, resulting in anchoring the PVP polymer chain to the Au surfaces. The complex facilitates Au ion reduction and Au nucleation to form stable AuNPs. Additionally, PVP surrounds the Au surface via physical and chemical bonding, which prevents contact between particles that can result in severe particle agglomeration. The UV-Vis spectra showed an intense peak, which indicates the SPR, that occurs as a unique phenomenon in plasmonic metal nanoparticles. It enhances all radiative properties, including scattering and absorption. The FT-IR results proved the formation of AuNPs and presence of the secondary metabolites on the surface of AuNPs. The crystallite size of AuNP was obtained 16.4 nm from the XRD analysis.

Free radicals can damage cells and cause mutations, which are harmful to human health. Antioxidants play a crucial role in protecting against this damage. The considerable antioxidant activity of the AuNPs can be attributed to the secondary metabolites of the *H. canaliculatum* extract. According to the study by Varamini et al. (2009), five quinoline alkaloids (7-Isopentenyloxy-γ-fagarine, Atanine, Skimmianine, Flindersine, and perfamine) have been identified in the methanolic extract of this plant. These secondary metabolites are known for their antioxidant properties and may contribute to the reduction and stabilization of AuNPs through adsorption onto their surface (Shabaani et al., 2020; Ghasemi et al., 2025). Additinally, the small size and large surface area of AuNPs also provide abundant active sites for the absorption of such bioactive compounds (Khan et al., 2019).

Conclusion

In the present study, we describe a novel, simple, and eco-friendly method for the synthesis of AuNPs using an aqueous extract of *H. canaliculatum*. The color change from yellow to purple during the reaction confirmed the formation of the AuNPs.

Moreover, the UV-Vis spectroscopy exhibited a surface plasmon resonance band at 523 nm, indicating the synthesis of the AuNPs. Also, the SEM image revealed particle sizes of 18-25 nm for the AuNPs, which showed an agreement with the particle size (16.4 nm) obtained by XRD analysis. Furthermore, FT-IR spectroscopy suggested the involvement of secondary metabolites, e.g., alkaloids, flavonoids, and phenolic compounds during the synthesis process. The as-prepared AuNPs presented significant inhibitory activity (86.33±1.86%) at the highest concentration (250 µg mL^{-1}) in the DPPH assay due to the surface covered by bioactive compounds. These results suggest a valuable strategy for preparing the biosynthesized AuNPs for pharmaceutical applications.

Supplementary Materials

No supplementary material is available for this article.

Author Contributions

Conceptualization, K. L.; methodology, K. L., L. G. and P. A.; investigation, N. A., K. L., L. G. and P. A.; formal analysis, N. A.; data curation, N. A.; writing—original draft preparation, L. G. and P. A.; writing—review and editing, L. G. and P. A.; supervision, K. L. All authors have read and agreed to the published version of the manuscript.

Funding

This research received no external funding.

Acknowledgments

Not applicable.

Conflict of Interest Statement

The authors declare no conflict of interest.

References

Abdelghany, A., Mekhail, M.S., Abdelrazek, E., and Aboud, M. (2015). Combined DFT/FTIR structural studies of monodispersed PVP/Gold and silver nano particles. *J. Alloys Compd.* 646: 326-332.

Alharbi, N.S., Bhakyaraj, K., Gopinath, K., Govindarajan, M., Kumuraguru, S., Mohan, S., Kaleeswarran, P., Kadaikunnan, S., Khaled, J.M., and Benelli, G. (2017). Gum-mediated fabrication of eco-friendly gold nanoparticles promoting cell division and pollen germination in plant cells. *J. Clust. Sci.* 28: 507-517.

Arzani, V., Soleimani, M., Fritsch, T., Jacob, U.M., Calabrese, V., and Arzani, A. (2025). Plant polyphenols, terpenes, and terpenoids in oral health. *Open Med.* 20(1): 20251183.

Boruah, J.S., Devi, C., Hazarika, U., Reddy, P.V.B., Chowdhury, D., Barthakur, M., and Kalita, P. (2021). Green synthesis of gold nanoparticles using an antiepileptic plant extract: in vitro biological and photo-catalytic activities. *RSC Adv.* 11(45): 28029-28041.

Chen, J., Li, Y., Fang, G., Cao, Z., Shang, Y., Alfarraj, S., Alharbi, S.A., Li, J., Yang, S., and Duan, X. (2021). Green synthesis, characterization, cytotoxicity, antioxidant, and anti-human ovarian cancer activities of *Curcumae kwangsiensis* leaf aqueous extract green-synthesized gold nanoparticles. *Arab. J. Chem.* 14(3): 103000.

Deghiedy, N., and El-Sayed, S. (2020). Evaluation of the structural and optical characters of PVA/PVP blended films. *Opt. Mater.* 100: 109667.

Fatima, Z., Saleem, R., Khan, R.R.M., Liaqat, M., Pervaiz, M., Saeed, Z., Muhammad, G., Amin, M., and Rasheed, S. (2024). Green synthesis, properties, and biomedical potential of gold nanoparticles: A comprehensive review. *Biocatal. Agric. Biotechnol.*: 103271.

Ghasemi, M., Govahi, M., and Litkohi, H.R. (2025). Green synthesis of silver nanoparticles (AgNPs) and chitosan-coated silver nanoparticles (CS-AgNPs) using Ferula gummosa Boiss. gum extract: A green nano drug for potential applications in medicine. *Int. J. Biol. Macromol.* 291: 138619.

Ismillayli, N., Suprapto, S., Santoso, E., Nugraha, R.E., Holilah, H., Bahruji, H., Jalil, A.A., Hermanto, D., and Prasetyoko, D. (2024). The role of pH-induced tautomerism of polyvinylpyrrolidone on the size,

stability, and antioxidant and antibacterial activities of silver nanoparticles synthesized using microwave radiation. *RSC Adv.* 14(7): 4509-4517.

Khan, Z.U.H., Sadiq, H.M., Shah, N.S., Khan, A.U., Muhammad, N., Hassan, S.U., Tahir, K., Khan, F.U., Imran, M., and Ahmad, N. (2019). Greener synthesis of zinc oxide nanoparticles using *Trianthema portulacastrum* extract and evaluation of its photocatalytic and biological applications. *J. Photochem. Photobiol.* 192: 147-157.

Kureshi, A.A., Vaghela, H.M., Kumar, S., Singh, R., and Kumari, P. (2020). Green synthesis of gold nanoparticles mediated by Garcinia fruits and their biological applications. *Pharm. Sci.* 27(2): 238-250.

Mahajan, M., Kumar, S., Gaur, J., Kaushal, S., Dalal, J., Singh, G., Misra, M., and Ahlawat, D.S. (2025). Green synthesis of ZnO nanoparticles using *Justicia adhatoda* for photocatalytic degradation of malachite green and reduction of 4-nitrophenol. *RSC Adv.* 15(4): 2958-2980.

Mohammadhosseini, M., Venditti, A., Frezza, C., Serafini, M., Bianco, A., and Mahdavi, B. (2021). The genus *haplophyllum* juss.: Phytochemistry and bioactivities—a review. *Molecules* 26(15): 4664.

Mohammadinejad, R., Shavandi, A., Raie, D.S., Sangeetha, J., Soleimani, M., Hajibehzad, S.S., Thangadurai, D., Hospet, R., Popoola, J.O., and Arzani, A. (2019). Plant molecular farming: production of metallic nanoparticles and therapeutic proteins using green factories. *Green Chem.* 21(8): 1845-1865.

Molyneux, P. (2004). The use of the stable free radical diphenylpicrylhydrazyl (DPPH) for estimating antioxidant activity. *Songklanakarin J. Sci. Technol.* 26(2): 211-219.

Nikbakht, M., Gholami, A., Morowvat, M., Ghasemi, Y., and Mohagheghzadeh, A. (2016). Analysis of volatiles and 18S rRNA gene of *Haplophyllum canaliculatum* in in vitro cultures. *Res. j. pharmacogn.* 3(4): 17-25.

Ortega-Cordova, R., Sanchez-Carillo, K., Carrasco-Saavedra, S., Ramírez-García, G., Perez-García, M.G., Soltero-Martínez, J.F.A., and Mota-Morales, J.D. (2024). Polyvinylpyrrolidone-mediated synthesis of ultra-stable gold nanoparticles in a nonaqueous choline chloride–urea deep eutectic solvent. *RSC Appl. Interfaces* 1(3): 600-611.

Patil, T.P., Vibhute, A.A., Patil, S.L., Dongale, T.D., and Tiwari, A.P. (2023). Green synthesis of gold nanoparticles via *Capsicum annum* fruit extract: characterization, antiangiogenic, antioxidant and anti-inflammatory activities. *Appl. Surf. Sci. Adv.* 13: 100372.

Rosyidah, A.l., Purbani, D.C., Pratiwi, R.D., Muttaqien, S.E., Nantapong, N., Warsito, M.F., Fikri, M.N., Ruth, F., Gustini, N., and Syahputra, G. (2024). Eco-friendly synthesis of gold nanoparticles by marine microalgae *Synechococcus moorigangae:* Characterization, antimicrobial, and antioxidant properties. *Kuwait J. Sci.* 51(2): 100194.

Saleh, T.A. (2022). "Properties of nanoadsorbents and adsorption mechanisms," in *Interface Sci. Technol.*: Elsevier), 233-263.

Santhosh, P.B., Genova, J., and Chamati, H. (2022). Green synthesis of gold nanoparticles: An eco-friendly approach. *Chemistry* 4(2): 345-369.

Shabaani, M., Rahaiee, S., Zare, M., and Jafari, S.M. (2020). Green synthesis of ZnO nanoparticles using loquat seed extract; Biological functions and photocatalytic degradation properties. *Lwt* 134: 110133.

Shehzad, A., Qureshi, M., Jabeen, S., Ahmad, R., Alabdalall, A.H., Aljafary, M.A., and Al-Suhaimi, E. (2018). Synthesis, characterization and antibacterial activity of silver nanoparticles using *Rhazya stricta*. *PeerJ* 6: e6086.

Sujitha, M.V., and Kannan, S. (2013). Green synthesis of gold nanoparticles using Citrus fruits (*Citrus limon*, *Citrus reticulata* and *Citrus sinensis*) aqueous extract and its characterization. *Spectrochim. Acta - A: Mol. Biomol. Spectrosc.* 102: 15-23.

Tharani, S., Bharathi, D., and Ranjithkumar, R. (2020). Extracellular green synthesis of chitosan-silver nanoparticles using *Lactobacillus reuteri* for antibacterial applications. *Biocatal. Agric. Biotechnol.* 30: 101838.

Varamini, P., Javidnia, K., Soltani, M., Mehdipour, A.R., and Ghaderi, A. (2009). Cytotoxic activity and cell cycle analysis of quinoline alkaloids isolated from *Haplophyllum canaliculatum* Boiss. *Planta Med.* 75(14): 1509-1516.

Wei, S., Lian, J., and Jiang, Q. (2009). Controlling growth of ZnO rods by polyvinylpyrrolidone (PVP) and their optical properties. *Appl. Surf. Sci. Adv.* 255(15): 6978-6984.

Zakaria, Z., Kamarudin, S., and Timmiati, S. (2019). Influence of graphene oxide on the ethanol permeability and ionic conductivity of QPVA-based membrane in passive alkaline direct ethanol fuel cells. *Nanoscale Res. Lett.* 14(1): 28.

Zidan, H.M., Abdelrazek, E.M., Abdelghany, A.M., and Tarabiah, A.E. (2019). Characterization and some physical studies of PVA/PVP filled with MWCNTs. *J. Mater. Res. Technol.* 8(1): 904-913.

JPMB
Journal of Plant Molecular Breeding
Published by Genetics and Agricultural Biotechnology Institute of Tabarestan
2025 | Volume 13 | Issue 1

مقاله پژوهشی

سنتز سبز نانوذرات طلا با استفاده از عصاره آبی گیاه سدابی ترکه‌ای و بررسی خواص آنتی اکسیدانی آن

نیلوفر احدی[۱]، کامبیز لاریجانی[۱]، لیدا قادری *[۲]، پروین آسن *[۳]

[۱] گروه شیمی، واحد علوم و تحقیقات، دانشگاه آزاد اسلامی، تهران، ایران
[۲] دانشکده گیاهان دارویی، دانشگاه تخصصی فناوری‌های نوین آمل، آمل ، ایران
[۳] گروه نانوزیست فناوری، دانشکده زیست فناوری، دانشگاه تخصصی فناوری‌های نوین آمل، آمل ۶۳۱۱۱ -۴۶۱۵۸، ایران

چکیده: امروزه سنتز سبز نانوذرات طلا به دلیل کاربردهای متنوع خود در زمینه‌های مختلف، محبوبیت قابل توجهی بدست آورده است. این مطالعه سنتز نانوذرات طلا را از طریق کاهش کلروآوریک اسید توسط عصاره آبی گیاه سدابی ترکه‌ای به عنوان عامل کاهنده و تثبیت‌کننده گزارش می‌کند. علاوه بر این، فعالیت آنتی‌اکسیدانی نانوذرات طلای سنتز شده به روش DPPH مورد بررسی قرار گرفته است. خواص فیزیکوشیمیایی نانوذرات طلا با طیف‌سنجی مرئی- فرابنفش (UV-Vis)، طیف‌سنجی تبدیل فوریه مادون قرمز (FT-IR)، پراش اشعه ایکس (XRD)، میکروسکوپ الکترونی روبشی گسیل میدانی (FESEM) مشخص شد. تصویر SEM نشان داد که اندازه نانوذرات طلا تقریبا بین ۱۸ تا ۲۰ نانومتر است که با اندازه ۱۶/۴ نانومتر تعیین شده توسط تجزیه و تحلیل XRD همخوانی دارد. علاوه بر این نانوذرات طلای سنتز شده، فعالیت آنتی اکسیدانی قابل توجهی را در آزمون DPPH به روش وابسته به غلظت از خود نشان داده است. نتایج بدست آمده، رویکرد امیدوار کننده‌ای را برای توسعه نانوذرات طلای بیوسنتز شده برای کاربردهای دارویی ارائه می‌دهد.

کلمات کلیدی: سنتز سبز، نانوذرات طلا، سدابی ترکه‌ای، فعالیت آنتی اکسیدانی.

ویراستار علمی
دکتر پوریا بی پروا،
گروه علوم پایه، دانشکده علوم زراعی، دانشگاه علوم کشاورزی و منابع طبیعی ساری، ساری

تاریخ
دریافت: ۲۸ فروردین ۱۴۰۴
پذیرش: ۲۴ اردیبهشت ۱۴۰۴
چاپ: ۱ خرداد ۱۴۰۴

نویسنده مسئول
دکتر لیدا قادری
l.ghaderi@ausmt.ac.ir
دکتر پروین آسن
parvinasen@ausmt.ac.ir

ارجاع به این مقاله
Ahadi, N., Larijani, K., Ghaderi, L., and Asen, P. (2025). Green synthesis of gold nanoparticles using aqueous extract of *Haplophyllum canaliculatum* Boiss and its antioxidant activity. *J Plant Mol Breed. 13* (1): 71-80.
doi: 10.22058/jpmb.2025.2058107.1336.